Automatic extraction of reduced-order models from CFD simulations for building energy modelling

Mullen, D. T., Keane, M. M., Geron, M., & Monaghan, R. F. D. (2015). Automatic extraction of reduced-order models from CFD simulations for building energy modelling. *Energy and Buildings*, *99*, 313-326. https://doi.org/10.1016/j.enbuild.2015.04.015

Published in:
Energy and Buildings

Document Version:
Peer reviewed version

Queen's University Belfast - Research Portal:
Link to publication record in Queen's University Belfast Research Portal

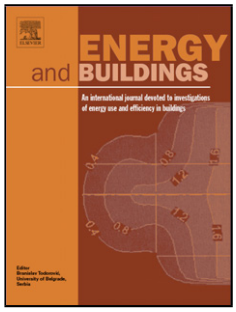

Title: Automatic extraction of reduced-order models from CFD simulations for building energy modelling

Author: D.T. Mullen M.M. Keane M. Geron R.F.D. Monaghan

PII: S0378-7788(15)00314-X
DOI: http://dx.doi.org/doi:10.1016/j.enbuild.2015.04.015
Reference: ENB 5807

To appear in: *ENB*

Received date: 3-9-2014
Revised date: 26-3-2015
Accepted date: 12-4-2015

Please cite this article as: D.T. Mullen, M.M. Keane, M. Geron, R.F.D. Monaghan, Automatic extraction of reduced-order models from CFD simulations for building energy modelling, *Energy and Buildings* (2015), http://dx.doi.org/10.1016/j.enbuild.2015.04.015

Highlights

- Validated CFD models were presented for an office space.
- A CFD-ROM Method to automatically extract reduced order models from CFD
- The extracted ROMs presents a total error lower than 5% with a solution time of 20s.

*Corresponding Author: Marco Geron, School of Mechanical and Aerospace Engineering, Queen's University Belfast, Belfast, UK. Tel:+442890424728. E-mail address: m.geron@qub.ac.uk

Automatic extraction of reduced-order models from CFD simulations for building energy modelling

D.T. Mullen[1,2], M.M. Keane[1,2] , M. Geron*[,3], R.F.D. Monaghan[1,2]
[1] National University of Ireland Galway – College of Engineering and Informatics – Ryan Institute
[2] National University of Ireland Galway – Informatics Research Unit for Sustainable Engineering (IRUSE)
[3] Queen's University Belfast – School of Mechanical and Aerospace Engineering

Abstract

Accurate modelling of the internal climate of buildings is essential if Building Energy Management Systems (BEMS) are to efficiently maintain adequate thermal comfort. Computational fluid dynamics (CFD) models are usually utilised to predict internal climate. Nevertheless CFD models, although providing the necessary level of accuracy, are highly computationally expensive, and cannot practically be integrated in BEMS. This paper presents and describes validation of a CFD-ROM method for real-time simulations of building thermal performance. The CFD-ROM method involves the automatic extraction and solution of reduced order models (ROMs) from validated CFD simulations. ROMs are shown to be adequately accurate with a total error below 5% and to retain satisfactory representation of the phenomena modelled. Each ROM has a time to solution under 20 seconds, which opens the potential of their integration with BEMS, giving real-time physics-based building energy modelling. A parameter study was conducted to investigate the applicability of the extracted ROM to initial boundary conditions different from those from which it was extracted. The results show that the ROMs retained satisfactory total errors when the initial conditions in the room were varied by ±5^{o}C. This allows the production of a finite number of ROMs with the ability to rapidly model many possible scenarios.

Keywords: Computational modelling, reduced order models, thermal comfort, energy efficient building, natural ventilation

1. Introduction

One of the most pressing issues facing society today is the increasingly expensive, polluting and insecure sources of energy available. Energy efficiency will play an ever-increasing role in ensuring sustainable energy use. Up to 40% of the world's energy is consumed in buildings, with 30-40% of that energy used in the maintenance of indoor thermal comfort [1], [2]. Thermal comfort is defined as "that condition of mind which expresses satisfaction with the thermal environment" [3], [4]. Field studies have been completed in order to establish governing conditions for thermal comfort [5]. These studies showed that the internal climate of a room is the strongest factor in maintaining thermal comfort. Direct manipulation of the internal climate is necessary to retain an acceptable level of thermal comfort. This manipulation is completed by

*Corresponding Author: Marco Geron, School of Mechanical and Aerospace Engineering, Queen's University Belfast, Belfast, UK. Tel:+442890424728. E-mail address: m.geron@qub.ac.uk

means of internal heating sources (radiators or convectors), internal cooling sources (air conditioning units) and natural ventilation (NV). The application of NV methods is of considerable importance as it is considered an efficient way to keep a healthy and comfortable environment while reducing energy consumption in buildings [6], [7]. In order for the above mentioned climate manipulation methods to be efficiently utilised they must be modelled and incorporated into Building Energy Management Systems (BEMS) strategies. The response of a room to NV actions, coupled with internal heating/cooling methods can be difficult to predict and thus must be correctly modelled [8]–[11].

Validated computational fluid dynamics (CFD) simulations [12], [13] have been successfully created and utilised to analyse thermal behaviour and user comfort of office space [14]–[17] in combination with wireless sensor networks (WSN) [18]. Although successful, these CFD simulations are computationally expensive, especially if unsteady simulations are required or if they are to be used in conjunction with BEMS for operational strategies. Reduced order models (ROMs) involve a representation of a given system/process by a mathematical model that is highly simplified or 'reduced', but still describes important aspects of the system/process [19]. In the past three decades different types of ROMs have been developed for predicting the thermo-fluid behaviour of building zones. The different models can be categorised according to the hypothesis adopted to describe the airflow distribution in the zones. The most simplified model, often utilised for energy loads calculations (e.g. Energy +) assumes the perfectly mixed hypothesis of the air distribution in the zone. This type of model has shown to be deficient when temperature stratification is present and must be simulated. A second, more complex model, utilised for modelling airflow in rooms is defined as thermo-fluid network model (or Compact Thermal Fluid Model). This model still considers uniform values of the different variables (e.g. temperature) at the nodes, but several nodes are introduced to describe temperature stratification and or plumes/jets [20] inside the zone. A third type of model is what is referred to as "zonal model". In this type of model the domain (room/zone) is divided into subzones and mass and energy conservation equations are solved throughout the different zones. This model can be considered as an intermediate model between the thermo-fluid network and more sophisticated CFD modelling tools. An extensive and exhaustive review of the zonal model approach can be found in Megri et al.[21].

Generalising it can be said that the generation of a reduced order model usually involves the division of the domain into a number of subzones. The number and size of the subzones depends on the level of accuracy required by the user. ROMs have been shown to have the potential for near real-time analysis [22] and can be a valid alternative for CFD models [23],[24] and [20]. The main challenges with the development of these models are (1) the decision on how to divide the domain into zones which is usually left to the experience of the researcher, and (2) the empirical data or correlations which need to be used to evaluate the parameters which characterise zone-to-zone energy and/or fluid exchange.

*Corresponding Author: Marco Geron, School of Mechanical and Aerospace Engineering, Queen's University Belfast, Belfast, UK. Tel:+442890424728. E-mail address: m.geron@qub.ac.uk

The focus of this research is thus to develop a CFD-ROM method that will facilitate the automatic extraction of ROM from validated CFD models. This is a concept which has previously been developed in the area of combustion [25]. As the data used to create the ROM is extracted directly from a CFD file, the use of empirical data and the reliance on user experience is greatly reduced. This paper will present the CFD-ROM method that has been developed over the course of the on-going research. The following sections will describe the CFD model used in the validation of the CFD-ROM method, provide a description how the CFD-ROM method functions and present the results generated over the course of the research. The results presented will include the validation of CFD models, the validation of the CFD-ROM method and a parameter study detailing the range of functionality of the CFD-ROM method.

2. Experimental data and CFD model

2.1 Experimental setup

The location for the study is a north-facing office in the Environmental Research Institute (ERI) building at University College Cork (UCC), Ireland. It is shown in Figure 1 and has dimensions 5.2 m x 5.6 m x 2.9 m. It is heated by two Dimplex SmartRad fan assisted convectors. Two electronically controlled windows are present and have a maximum aperture of 20^o. Furniture comprises five sets of desks and chairs, and shelf units. No additional heating or momentum sources are present at the time of the experiments, for example computers and people. A set of 35 wireless temperature sensors (TelosB), with a measurement accuracy of $\pm 0.5\ ^oC$, are deployed at three different levels in the office space: 5 at ceiling level (2.65 m above floor), 20 at user level (1 m above floor) and 10 at floor level (0.2 m above floor) as shown in Figure 2. The measurements obtained from the sensors of this WSN have been utilised to validate the different CFD simulations.

The temperature of the east and west facing walls are measured at one location by temperature sensor TMC6-HE [26]. The temperature of the ceiling and of the floor were measured at a central location by temperature sensors TMC20-HD [26]. Both sensors have an accuracy of $\pm 0.25\ ^oC$.

The anemometers, which have an accuracy of ±0.05 m/s or 1% of full scale, are positioned in front of the opened windows to evaluate the air velocity component normal to the opening and on top of the convectors. Three different elements are considered and deemed as the most influential in characterising the flow features in the office space: the convectors, the windows and the door. The convectors are modelled at maximum mass flow rate only (0.044 kg/s), and windows and door are open at angles of 20^o and 90^o, respectively.

2.2 CFD Model

*Corresponding Author: Marco Geron, School of Mechanical and Aerospace Engineering, Queen's University Belfast, Belfast, UK. Tel:+442890424728. E-mail address: m.geron@qub.ac.uk

The Phoenics CFD software [27] has been utilised to generate a database of test cases utilised both for the generation and the testing of ROMs. For all the CFD simulations the flow has been deemed turbulent and the steady-state Reynolds Average Navier-Stokes (RANS) approach coupled with the Re-Normalisation Group (RNG) k-ε turbulence model has been utilised to model the fluid flow. Air has been modelled as an incompressible ideal gas. Due to the immersed body technique utilised by Phoenics to deal with object in the domain, a Cartesian structured grid with 1,572,165 cells (115x147x93) was utilised to discretise the zone of interest. Constant temperature boundary conditions have been utilised for the ceiling, the floor, and east and west walls of the room. On the south-facing wall an adiabatic boundary condition was applied. This choice was justified both by IR pictures shot during the experiments and by consideration of the unchanged temperature registered on the corridor in contact with that wall. On the north facing wall an adiabatic boundary condition was applied to all wooden panels while an overall heat transfer coefficient of U = 1 W/m^2K was applied to the triple glazed panels. When this boundary condition was imposed the outdoors temperature was utilised as reference temperature. All the other objects in the room (desks and chairs) were considered as adiabatic. The door, when opened, was modelled as a zone of constant pressure; this assumption was confirmed by on-site pressure measurements. The convectors were modelled using two surfaces: an inlet surface at the top of the convectors, where mass flow rate (0.044 kg/s) and temperature (45 ^oC) were imposed, and an outlet surface at the bottom of the convectors, where an extraction mass flow rate equal to the inlet mass flow rate was imposed. Opened windows were also modelled as inlet surfaces with an imposed normal velocity, which ranges from 0.2 m/s to 0.5 m/s and temperature which for the cases considered varied between 4 ^oC and 14 ^oC. The flow direction on the two windows was monitored through all the experiments by the mean of two small flags, which confirmed that the two windows were always acting as inlets. Through a portable velocity sensor (OMNIPORT 20) it was also noticed that in the last 20% of the window opening the airflow was quite small. For this reason a surface contraction coefficient equal to 0.8 was imposed at the window inlet boundary condition. This decreased the overall flow rate of a 20%.

2.3 Validation of CFD simulations

All CFD simulations developed have been checked for grid convergence and validated with experimental data obtained from the WSN as shown in Figure 3 and Figure 5. The course (N_{fine} = 1,572,165 cells) and fine (N_{coarse} = 568,260 cells) grids utilised for the grid convergence analysis differ according to a refinement ratio $r = \left(\frac{N_{fine}}{N_{coarse}}\right)^{1/3} = 1.4$. Wall functions were utilised to model the thermal and velocity boundary layer, for this reason a Y+ around 100 was sought for the coarse mesh and a Y+ around 50 was sought on the fine mesh. The turbulence model utilised was the RNG k-ε model which has proven to perform well for this type of flow [28]. Experiments were run for 6 to 8 hours. The choice of 6 to 8 hours was made in order to guarantee enough time for the air temperature to reach a "quasi" steady state and to have enough data to evaluate average and standard deviations of the recorded values. The definition of "quasi" steady state

*Corresponding Author: Marco Geron, School of Mechanical and Aerospace Engineering, Queen's University Belfast, Belfast, UK. Tel:+442890424728. E-mail address: m.geron@qub.ac.uk

derives from the effect of thermal inertia for the ceiling and the room floor that the authors noticed when running the experiments. It was noticed in fact that the rate of change of the temperature of the ceiling and of the floor often lagged behind, as shown in Figure 4, and that an actual steady state was never reached. Nevertheless experiments were deemed at "quasi" steady state when 10-minute temperature variation was < 1%. At quasi steady state, average values and standard deviations were evaluated for the 35 sensors. Figure 5 shows the comparison between the experimental data and the CFD predictions for four cases, which are described in later sections. The band of error reported for the experimental data includes the measurement uncertainty (standard deviation) and sensor accuracy. It is possible to assert that a satisfactory agreement is seen between experimental and the numerical data indicating that the CFD simulations properly represent the flow features which develop in the office space under different boundary conditions. The CFD simulation can thus be reliably utilised to generate ROMs.

3. CFD-ROM Method

3.1 Method overview

As can be seen from Figure 6 the CFD-ROM method functions in conjunction with validated CFD models and allow the BEMS to rapidly model a variety of different model parameters for a given ROM. This rapid modelling ability allows the BEMS to predict the thermal response of any action to change the environment within the range of functionality of the ROM being used.

The method under development consists of a Python script that automatically extracts a ROM from a CFD solution file. All CFD files used during the development of the CFD-ROM method were outputted from the CFD package in Tecplot [29] format. Tecplot is widely used for the visualisation of CFD simulations and this format was chosen because CFD files exported in this way follow a standard layout that is a widely available export option for CFD packages. This increases the versatility of the CFD-ROM method and ensures a standard input format. The python script consists of five sections of code shown in Figure 7, which are (1) structured-to-unstructured mesh converter, (2) pre-processer, (3) zone generator, (4) zone interactions and boundary conditions calculator, and (5) SINDA/FLUINT [30] input file generator. These sections are described in detail in the following sections. After the ROM is generated it is solved using SINDA/FLUINT, a finite-difference, lumped parameter tool for heat transfer design and fluid flow modelling.

3.2 Structured-to-unstructured mesh converter

A CFD mesh can be generated as either structured or unstructured. A structured mesh is comprised of hexahedron elements that follow a uniform pattern. An unstructured mesh does not follow a uniform pattern, and can be comprised of various element types [31]. For maximum flexibility, the CFD-ROM method uses

*Corresponding Author: Marco Geron, School of Mechanical and Aerospace Engineering, Queen's University Belfast, Belfast, UK. Tel:+442890424728. E-mail address: m.geron@qub.ac.uk

unstructured mesh as input. The sole difference between unstructured and structured meshes in CFD solution files is that an unstructured mesh contains a connectivity array.

The structured-to-unstructured mesh converter reads a structured mesh of a CFD domain and outputs a connectivity array. Each entry in this array is 8 numbers in length and lists the nodes present in each element in the domain. If the element in question has less than 8 nodes one or more of the nodes is repeated in the entry. The converter uses the geometric position of the structured grid to define which nodes are present in each element in the domain and outputs the array in the required form.

3.3 Pre-processor

The pre-processing section of the code is used to perform any operations that are not ROM specific and thus only have to be performed once per CFD simulation. The main functions performed in this section are to (1) create the element connections array (an array in which each entry lists every element connected to another element in the domain by at least one node), (2) define inlet and outlet elements, and (3) calculate the volume of each element. These functions are complex operations, which require substantial processing power, so performing them only once in the pre-processer improves the computational efficiency of ROM extraction.

3.4 Zone generator

In this section the fluid domain is separated into the number of zones as defined by the user. In order to describe the zone generator, four key definitions are introduced: zoning criterion, criterion increment, zone-type and zone. Examples of the application of these definitions are shown in Figure 8. A zoning criterion is a physical property, such as temperature, velocity, carbon dioxide concentration or geometric position, whose local value is used to define zones within the simulation domain. The range of each zoning criterion is defined by its minimum and maximum values in the simulation domain. In the work presented here, and in Figure 8, the only zoning criterion used is temperature. A criterion increment is the magnitude of the range of the zoning criterion that defines a zone. Values of criterion increment are calculated by the zone generator based on how many zones are required by the user. Figure 8 shows criterion increments for temperature of 2 ^{o}C, as shown in panels (a)-(c), and 1 ^{o}C, as shown in panels (d)-(f). A zone-type is defined by the total volume within the simulation domain whose values of zoning criteria fall within a defined range of a criteria increment. Panels (b) and (e) in Figure 8 show sample zone-types generated by temperature increments of 2 ^{o}C and 1^{o}C, respectively. As shown in the figure, multiple distinct locations within the simulation domain can have the same zone-type. A zone is defined as a unique, spatially distinct volume within the simulation domain that consists of one zone-type only. This is illustrated in Figure 8 (b) and (c) for a temperature increment of 2 ^{o}C. Panel (b) shows that there are two distinct regions of zone-type 3 for this example. While

*Corresponding Author: Marco Geron, School of Mechanical and Aerospace Engineering, Queen's University Belfast, Belfast, UK. Tel:+442890424728. E-mail address: m.geron@qub.ac.uk

temperature may be similar in these two zone-types, the same cannot necessarily be said for other properties that were not used for zone generation. Therefore the two distinct regions of zone-type 3 are split into two unique zones (3 and 4), as shown in panel (c). The difference between zone-type and zone is similarly illustrated for a temperature increment of 1 ^{o}C in Figure 8 (e) and (f). Six zone-types are shown in panel (e), of which two (4 and 5) consist of two distinct regions. These zone-types are therefore split into two unique zones each; zone-type 4 forming zones 3 and 5, and zone-type 5 forming zones 4 and 7. Physical properties within a zone are calculated from the mass-weighted average over the computational nodes that comprise the zone.

The operations performed in this section are complex and are described graphically in Figure 9. The maximum number of zones generated is user-defined to represent the level of accuracy required for the application. This is sole step in the CFD-ROM process that requires user experience and know-how. The number of zones to be generated determines the zone criteria increments employed by the process. A zone is created by initially taking one element that has not already been assigned to a zone and which also falls within the current zone-type range. One zone-type may have more than one zone associated with it. A check is then performed to determine which of its connected elements are also within the zone-type range and the applicable elements are added to the zone. The process is then repeated for the newly-added elements until no further elements that meet the required criteria can be found. Once this occurs, the zone has been fully defined.

An important factor to note with the method is that the zone generation is an iterative process. The zoning process starts by generating the number of zones associated with the minimum number of zones-types, which is always two. The program then checks if the minimum number of zones as defined by the user has been created. If the number of zones produced is less than the minimum requirement, the code repeats the zoning process for the next number of zone-types (four) and repeats the check. If during this iteration the minimum number of zones has been met the code returns the defined zones and continues to the next section. Otherwise it will continue to the next number of zone-types. Figure 10 shows the path that the zone generation may take for a certain input file. In this case the minimum number of zones is set to six.

3.5 Zone interactions and boundary conditions calculator

Once the zones have been defined the next section in the ROM extraction method is to determine how the zones interact with each other and to define the boundary conditions applied to the model. This method assumes that energy is transferred between the zones by means of convection, so the mass flow rates between zones are calculated. During the zoning section two arrays are generated: (1) the zone element array and (2) the zone number array. The entries in each array list details of the elements that are connected to

*Corresponding Author: Marco Geron, School of Mechanical and Aerospace Engineering, Queen's University Belfast, Belfast, UK. Tel:+442890424728. E-mail address: m.geron@qub.ac.uk

elements in different zones. These arrays are used in the calculation of the mass flow rates as they represent the elements that are on the boundary between zones.

In order to calculate the mass flow rates between zones the program iterates over each element in a zone-zone interface as illustrated in Figure 11. Each iteration calculates the area of contact between each pair of elements, the normal component of the CFD-predicted velocity to the area of contact and the average density. The mass flow rate is then evaluated using Equation 1 to Equation 3.

$$V = \left[V_x, V_y, V_z\right] \quad \text{Equation 1}$$

$$V_n = V.\vec{n} \quad \text{Equation 2}$$

$$\dot{m} = \rho A V_n \quad \text{Equation 3}$$

In these equations, V_x, V_y, and V_z are the x, y and z components of velocity, $\vec{n}$ is the normal vector to the element face, ρ is the density of the fluid, A is the area of contact between element faces and V_n is the component of velocity normal to the plane. Once this operation is completed for each element in a zone-zone interface the total mass flow rates is taken to be the sum over that interface.

The boundary conditions that are required for the ROM solver include domain wall temperatures (T), convection coefficient (h) at the domain walls, and inlet/outlet mass flow rates ($\dot{m}$) and temperatures. Whether an element is on the boundary of the domain has been previously established geometrically in the pre-processor. The average wall temperature is found by averaging the temperature of all elements in a boundary present in each zone. In order to calculate the convection coefficient over the wall, a flat plate forced turbulent convection correlation is used, as shown in Equation 4 to Equation 6.

$$\mathrm{Re}_L = u_L L / \nu \quad \text{Equation 4}$$

$$Nu_L = 0.037\,\mathrm{Re}_L^{4/5}\,\mathrm{Pr}^{1/3} \quad \text{Equation 5}$$

$$h = Nu_L k / L \quad \text{Equation 6}$$

In these equations, Re_L and Nu_L are the Reynolds and Nusselt numbers of the zone considered. The velocity u_L is the average fluid velocity of the zone, L is the characteristic length of the zone, ν is the kinematic viscosity, Pr is the Prandtl number (Pr = 0.71), and k is the thermal conductivity of the fluid. In order to find the location of the inlets and outlets of the model a mass flow rate balance was completed on each element during the pre-processer. This data was used to calculate the mass flow rate entering or leaving each of the zones and the temperature associated with the flow. Forced convection correlations were used

*Corresponding Author: Marco Geron, School of Mechanical and Aerospace Engineering, Queen's University Belfast, Belfast, UK. Tel:+442890424728. E-mail address: m.geron@qub.ac.uk

for this function as opposed to direct extraction of the heat transfer coefficient from the CFD solutions. Free convection was omitted from the calculations as it was determined to be minimal, in the scenarios analysed, when compared to the effects of forced convection.

3.6 SINDA/FLUINT input file generator

The last section of code in the ROM extraction method creates the input file for the ROM solver, SINDA/FLUINT. This involves writing the information generated from the previous steps in a file of the form required by the solver. SINDA/FLUINT iteratively solves dynamic or steady-state conservation equations for mass and energy for each zone in the ROM, using the boundary conditions extracted from the CFD simulation. Only steady-state modelling results using the energy conservation equation, which is given by Equation 7, are presented in this work. In this equation for the temperature of zone i (T_i), the first term on the right represents convection heat transfer with an adjacent wall, as described in Section 3.5, in which h_i is the local convection coefficient calculated from Equation 6, A_i is the wall-to-zone contact area and $T_{w,i}$ is the wall temperature that bounds zone i. For zones that do not touch any walls, this term is neglected. The second term on the right is the flow of enthalpy into zone i due to mass flow rates $\dot{m}_{j,i}$ from N_{in} other zones at temperatures T_j. Temperature-dependent polynomial expression for specific heat capacity (c_p) is integrated from a reference temperature T^0. The last term is the flow of enthalpy from zone i to other zones due to total zone mass flow rate $\dot{m}_i$. Imposition of steady-state mass conservation dictates that $\sum_{j=1}^{N_{in}} \dot{m}_{j,i} = \dot{m}_i$, as shown below. The fluid velocity field, which describes the velocities of the zone-to-zone flows, is not calculated by SINDA/FLUINT. Its values are fixed from the CFD simulation results, as described in Section 3.5. Steady-state zone temperatures are calculated iteratively, with the ideal gas equation of state used to resolve zone density. A fixed value of thermal conductivity (k) and a polynomial function of c_p in terms of temperature are used to model thermal properties of air. Enthalpy flows leaving zones are calculated by the energy conservation equation and used as inputs for downstream zones, in which zone temperature and exit enthalpy flows are calculated. Iteration is terminated when the overall error in global energy conservation is less than 10^{-6}.

$$0 = h_i A_i \left(T_{w,i} - T_i\right) + \sum_{j=1}^{N_{in}} \left(\dot{m}_{j,i} \int_{T^0}^{T_j} c_p dT \right) - \dot{m}_i \int_{T^0}^{T_i} c_p dT \qquad \text{Equation 7}$$

where $\sum_{j=1}^{N_{in}} \dot{m}_{j,i} = \dot{m}_i$ and $c_p = a + bT + cT^2 + dT^3 + eT^{-2}$

4. Results and Discussion

*Corresponding Author: Marco Geron, School of Mechanical and Aerospace Engineering, Queen's University Belfast, Belfast, UK. Tel:+442890424728. E-mail address: m.geron@qub.ac.uk

The following results are generated using the ROM extraction method described above. The data used in the extraction is taken from the previously-validated CFD model of the office space previously described. All the ROMs used to obtain the results are automatically extracted with the only input from the user being the minimum required number of zones. The total error, E_t, is computed to assess accuracy of the results. E_t is calculated using Equation 8 and Equation 9 and represents the error associated with the extraction and solution of the ROM based on ^{o}C values.

$$E_i = \frac{T_{CFD_i} - T_{ROM_i}}{T_{CFD_i}} \qquad \text{Equation 8}$$

$$E_t = \sum_{i=1}^{N_E} \frac{V_i |E_i|}{V_{domain}} \qquad \text{Equation 9}$$

In Equation 8 and Equation 9, T_{CFDi} is the temperature of element i predicted by the CFD solution, T_{ROMi} is the predicted temperature of the same element i when the zone temperature from the ROM solution is re-assigned to the original element. V_i is the volume of element i, V_{domain} is the total domain volume and N_E is the total number of elements in the domain. All contour plots shown are generated using the visualisation software Tecplot. Each contour plot shows x, y and z planes of the domain, with each plane passing through the centre of the domain.

4.1 ROM size independence study

A ROM size independence study was carried out for the complex scenario characterised by windows and door open and convectors on. The purpose is to determine the effect of larger ROM networks on the results considering both accuracy of the ROM and solution time. From Figure 12 to Figure 15 it can be seen that as the number of zones in a ROM increases, E_t decreases and stabilises, meaning the solution approaches that of the CFD simulation. Figure 16 shows the impact of ROM size on E_t and time to solution. E_t is seen to decrease with ROM size from 2.5% for 3 zones to 0.6% for 33 zones. This range of error was deemed acceptable for the required application. More important than the absolute value of E_t is the fact that ROM size independence is achieved in the range 10-30 zones as indicated by the stabilization of E_t as the ROM size increases. Based on the results from this size independence study a ROM size of 17-18 zones was chosen for use with all other extracted ROMs. Figure 16 also shows that time to solution increases with ROM size, this is to be expected with the increased numerical complexity of a larger ROM. The maximum ROM time to solution for this work is 20 seconds.

4.2 Parameter study

*Corresponding Author: Marco Geron, School of Mechanical and Aerospace Engineering, Queen's University Belfast, Belfast, UK. Tel:+442890424728. E-mail address: m.geron@qub.ac.uk

An important function of the CFD-ROM method is the ability to accurately predict a range of room conditions from a single ROM. This dramatically reduces the number of CFD simulations necessary to model all the possible scenarios for the internal conditions of the environment in question. In order to establish the range of functionality of a ROM generated using the CFD-ROM method, a parameter study is conducted by comparing the two ROM extraction approaches shown in Figure 17 and described below.

Multi-CFD approach

This ROM extraction approach involves extracting and solving one ROM for every CFD simulation. Each ROM describes only the room conditions as they are in the CFD simulation from which it was extracted. Although this method produces highly accurate ROMs, it is computationally inefficient as numerous CFD simulations have to be solved, which defeats the time-saving purpose of the CFD-ROM method. Results for this approach are shown for the purpose of comparison with the more practically useful Multi-ROM approach, which is described below. The total error based on ^{o}C values (E_t) for this approach is calculated using Equation 8 and Equation 9 as described above as the ROMs are produced using the same method as those used in the size independence study.

Multi-ROM approach

This ROM extraction approach involves solving numerous ROMs from one CFD simulation. This is the envisioned practical use for the CFD-ROM method. An appropriate CFD simulation is chosen, which represents the commonly-encountered conditions in the domain for a given configuration. A ROM is extracted from this simulation and the boundary conditions of the ROM are modified to represent the required conditions before the ROM is solved. This approach is highly computationally efficient as the number of CFD simulations is drastically reduced but it is potentially less accurate than the Multi-CFD approach. This potential reduction in accuracy occurs because the fluid flow field of the domain will change depending on the boundary conditions applied. The flow field of a ROM is fixed once generated, which leads to deviations from comparable CFD solutions.

E_t is calculated for the Multi-ROM approach by modifying Equation 8 to compare the solutions of the ROMs extracted using the Multi-ROM approach with the CFD simulations that they are attempting to replace (see Equation 10). Equation 10 is then used in conjunction with Equation 11 to calculate E_t.

$$E_j = \frac{T_{CFD,N_j} - T_{ROM,XN_j}}{T_{CFD,N_j}} \qquad \text{Equation 10}$$

$$E_t = \sum_{j=1}^{N_E} \frac{V_j \left| E_j \right|}{V_{domain}} \qquad \text{Equation 11}$$

*Corresponding Author: Marco Geron, School of Mechanical and Aerospace Engineering, Queen's University Belfast, Belfast, UK. Tel:+442890424728. E-mail address: m.geron@qub.ac.uk

Where, $T_{CFD,Nj}$ is the temperature of element j predicted by CFD solution N that the ROM is attempting to mimic, $T_{ROM,XNj}$ is the predicted temperature of element j from the ROM extracted from CFD solution X using the boundary conditions for CFD solution N, V_j is the volume of element j, V_{domain} is the total domain volume and N_E is the total number of elements in the domain.

The focus of this parameter study is to determine how accurately a ROM extracted using the Multi-ROM approach can predict a variety of room conditions. This is done by finding the difference in error based on ^oC values for each element in the domain between a ROM extracted using the Multi-CFD approach ($E_{i,ROM,N}$) with its Multi-ROM counterpart ($E_{i,ROM,XN}$). The error associated with the Multi-ROM approach (E_{MR}) is defined as the sum of the weighted difference between the two errors and calculated using Equation 12 to Equation 14.

$$E_{i,ROM,N} = \frac{T_{CFD_i} - T_{ROM_i}}{T_{CFD_i}} \quad \text{Equation 12}$$

$$E_{i,ROM,XN} = \frac{T_{CFD,N_i} - T_{ROM,XN_i}}{T_{CFD,N_i}} \quad \text{Equation 13}$$

$$E_{MR} = \sum_{i=1}^{N_E} \frac{V_i \left| E_{i,ROM,N} - E_{i,ROM,XN} \right|}{V_{domain}} \quad \text{Equation 14}$$

For this analysis, the variables used to complete the parameter study are the inlet air temperature of convectors (T_C) and windows (T_W). As the inlet air temperature from the door (T_D) is difficult to control in practical situations, modification of the door temperature is omitted from the parameter study. Four possible configurations of the previously-described office are analysed and described below.

- C1W0D0 - Convectors on, Windows closed, Door closed.
- C0W1D1 - Convectors off, Windows open, Door open.
- C1W0D1 - Convectors on, Windows closed, Door open.
- C1W1D1 - Convectors on, Windows open, Door open.

The matrix of CFD simulations produced for each case, their applied boundary conditions, and values of E_t for the ROMs produced using the Multi-CFD approach is shown in Table 1. The convector flow and window flow temperatures are varied ±5 ^oC around their base values. This size of variation is chosen

*Corresponding Author: Marco Geron, School of Mechanical and Aerospace Engineering, Queen's University Belfast, Belfast, UK. Tel:+442890424728. E-mail address: m.geron@qub.ac.uk

because (i) a 10 ^{o}C total temperature difference is significant in normal indoor environments, and (ii) the CFD-ROM method does not propose to have one CFD simulation encompass all potential indoor conditions, but rather to reduce the number of CFD simulations needed.

Table 2 shows the comparison between the E_t of all ROMs extracted using the Multi-CFD method and the Multi-ROM method, and the error associated with the Multi-ROM approach (E_{MR}). As expected, ROMs extracted using the Multi-ROM approach consistently resulted in a higher E_t than their Multi-CFD counterparts, with one exception. While higher, E_t is under 10% for each case with an average value of 6.22%. When compared to the respective Multi-CFD prediction, an average E_{MR} of 5.57% was seen. The range of E_{MR} seen (1.42%-8.43%) corresponds to an experimental error in temperature of between 0.26 ^{o}C and 1.64 ^{o}C with an average of 1.13 ^{o}C. Three cases were chosen which best represent the spread of E_{MR} over all the test cases.

1. C1W0D1 (T_C + 5^{o}C) → E_{MR} = 1.42%
2. C1W1D1 (T_w - 5^{o}C) → E_{MR} = 4.94%
3. C0W1D1 (T_w - 5^{o}C) → E_{MR} = 8.33%

Contour plots of E_{MR} for each case chosen are shown in Figure 18 to Figure 20. Iso-surfaces are shown where applicable to highlight areas of increased error. The first case chosen, C1W0D1 (T_C + 5^{o}C), shown in Figure 18, represents an optimum result in the Multi-ROM approach with an E_{MR} lower than 1.5%. The local difference error (E_{iMR}= $\left| E_{iROM\_N}-E_{iROM\_XN} \right|$) is low and appears to be concentrated toward the south side of the room close to the door. This is believed to be consequence of not varying the mass flow rates at the door boundary condition in the Multi-ROM approach.

The second case C1W1D1 (T_w-5^{o}C), in which the windows are closed and the door is open, shown Figure 19, shows a middle range E_{MR} of 4.94%. Similar to the first case, higher values of local error are apparent around the mass flow rate sources. The highest local error values surround the windows and to a lesser extent around the convectors. Moderate asymmetry can be seen for this case, this is believed to be due to the influence of the mass flow rate from the door.

The third case C0W1D1 (T_w-5^{o}C), in which windows and door are open, shown in Figure 20, represents the one of the worst case scenarios with an E_{MR} of 8.33%. Local error is highly concentrated around both open windows and is relatively low elsewhere. A region of high local error can be seen originating from the windows and extending along the floor. This path of local error follows the flow of cold air from the windows. This is due to the fact that the flow profile of the domain changed with the modified boundary conditions. The flow profile of ROMs is fixed once created which leads to these higher levels of error for certain conditions.

*Corresponding Author: Marco Geron, School of Mechanical and Aerospace Engineering, Queen's University Belfast, Belfast, UK. Tel:+442890424728. E-mail address: m.geron@qub.ac.uk

5. Conclusion

A method to automatically extract ROMs from a CFD solution has been presented and validated. The CFD-ROM method has been shown to have the ability to automatically extract ROMs from a converged and previously-validated CFD solution. The method retains a high level of accuracy, with a total error of 0.6% for a size-independent ROM consisting of 33 zones. Furthermore, it is highly computationally efficient, with a maximum time to solution of 20 seconds, compared to 5-8 hours for comparable CFD simulations. This time to solution enables ROMs to be used in the development and maintenance of a BEMS with the possibility for real-time building energy modelling.

A parameter study was completed to compare two different ROM extraction approaches; (1) direct extraction of one ROM per CFD solution (Multi-CFD), and (2) extraction of multiple ROMs from a single CFD solution, in which the applied boundary conditions to each ROM are changed to specify different internal conditions of the environment (Multi-ROM). Four specific cases for the room were analysed with a total of 24 ROMs generated. The results from this parameter study show an average total error, E_t, of 2.61% for ROMs extracted using the Multi-CFD approach. The same ROMs when generated using the Multi-ROM approach resulted in an average E_t of 6.22%. This corresponds to an average error associated with the use of the Multi-ROM approach, E_{MR}, of 5.57%. These results indicate that a ROM produced using the Multi-ROM approach provides the capability to predict the thermal response of a system to a satisfactory level of accuracy.

At present the work is focused on further developing the CFD-ROM method to increase its functionality and versatility. Short term work will focus on increasing the accuracy of ROMs produced using the Multi-ROM approach. Future development will involve developing a procedure for incorporating the ability for the user to vary the mass flow rates entering or leaving the system and incorporate the response of the domain when users are present in the office space.

6. Acknowledgements

The authors wish to acknowledge support for this work from the NUI Galway Millennium Fund for Research.

7. Nomenclature

A	Area of an element face (m^2)
CFD N	Numbered (N) CFD solution

*Corresponding Author: Marco Geron, School of Mechanical and Aerospace Engineering, Queen's University Belfast, Belfast, UK. Tel:+442890424728. E-mail address: m.geron@qub.ac.uk

E_i	An element within the CFD domain
$E_{iROM\ N}$	Error of a Multi-CFD extracted element (E_i)
$E_{iROM\ XN}$	Error of a Multi-ROM extracted element (E_i)
E_{MR}	Total error associated with the Multi-ROM approach (%)
E_t	Total error (%)
h	Convection coefficient (W/ m^2K)
k	Thermal conductivity (W/mK)
L	Characteristic length (m)
$\dot{m}$	Mass flow rate (kg/s)
$\vec{n}$	Normal vector to a plane
Nu_L	Nusselt number
Pr	Prandtl number
Re_L	Reynolds number
ROM N	Reduced order model extracted using the Multi-CFD approach
ROM XN	Reduced order model extracted using the Multi-ROM approach
T_{CFD_i}	Temperature of an element from the CFD solution (^oC or K)
T_{ROM_i}	Temperature of and element from the ROM solution (^oC or K)
u_∞	Fluid velocity (m/s)
V_{Domain}	Domain volume (m^3)
V_i	Zone volume (m^3)
V_n	Normal component of velocity (m/s)
V_x, V_y, V_z	X, Y and Z components of velocity respectively (m/s)
ρ	Density (kg/m^3)
ν	Kinematic viscosity (m^2/s)

8. References

[1] "U.S. Energy Information Administration (EIA)."

[2] L. Pérez-Lombard, J. Ortiz, and C. Pout, "A review on buildings energy consumption information," *Energy Build.*, vol. 40, no. 3, pp. 394–398, Jan. 2008.

[3] Ashrae, W. A. Dunn, G. S. Brager, K. A. Brown, D. R. Clark, J. J. Deringer, J. J. Hogeling, D. Int-hout, B. W. Jones, J. N. Knapp, A. G. Kwok, H. Levin, A. K. Melikov, P. Simmonds, J. M. Sipes, E. M. Sterling, and B. P. Sun, "ASHRAE STANDARD Thermal Environmental Conditions for Human Occupancy," vol. 2004, 2004.

*Corresponding Author: Marco Geron, School of Mechanical and Aerospace Engineering, Queen's University Belfast, Belfast, UK. Tel:+442890424728. E-mail address: m.geron@qub.ac.uk

[4] ISO, "ISO 7730: Ergonomics of the thermal environment Analytical determination and interpretation of thermal comfort using calculation of the PMV and PPD indices and local thermal comfort criteria," 2005.

[5] J. F. Nicol and M. A. Humphreys, "Adaptive thermal comfort and sustainable thermal standards for buildings," *Energy Build.*, vol. 34, no. 6, pp. 563–572, Jul. 2002.

[6] H. B. Rijal, P. Tuohy, M. A. Humphreys, J. F. Nicol, A. Samuel, and J. Clarke, "Using results from field surveys to predict the effect of open windows on thermal comfort and energy use in buildings," *Energy Build.*, vol. 39, no. 7, pp. 823–836, Jul. 2007.

[7] I. A. Raja, J. Nicol, and K. McCartney, "Natural ventilated buildings: Use of controls for changing indoor climate," *Renew. Energy*, vol. 15, no. 1–4, pp. 391–394, Sep. 1998.

[8] G. Tan and L. R. Glicksman, "Application of integrating multi-zone model with CFD simulation to natural ventilation prediction," *Energy Build.*, vol. 37, no. 10, pp. 1049–1057, Oct. 2005.

[9] S. D. Ray, N.-W. Gong, L. R. Glicksman, and J. A. Paradiso, "Experimental characterization of full-scale naturally ventilated atrium and validation of CFD simulations," *Energy Build.*, vol. 69, pp. 285–291, Feb. 2014.

[10] P. Heiselberg, S. Murakami, and C. Roulet, "Ventilation of large spaces in buildings," *Final Rep. IEA Annex*, 1998.

[11] Y. Jiang and Q. Chen, "Study of natural ventilation in buildings by large eddy simulation," *J. Wind Eng. Ind. Aerodyn.*, vol. 89, no. 13, pp. 1155–1178, Oct. 2001.

[12] D. Amsallem, J. Cortial, and C. Farhat, "Towards Real-Time CFD-Based Aeroelastic Computations Using a Database of Reduced-Order Information," pp. 1–26.

[13] H. B. Awbi, "Application of computational fluid dynamics in room ventilation," *Build. Environ.*, vol. 24, no. 1, pp. 73–84, Jan. 1989.

[14] T. Catalina, J. Virgone, and F. Kuznik, "Evaluation of thermal comfort using combined CFD and experimentation study in a test room equipped with a cooling ceiling," *Build. Environ.*, vol. 44, no. 8, pp. 1740–1750, 2009.

[15] W.-H. Chiang, C.-Y. Wang, and J.-S. Huang, "Evaluation of cooling ceiling and mechanical ventilation systems on thermal comfort using CFD study in an office for subtropical region," *Build. Environ.*, vol. 48, pp. 113–127, 2011.

[16] M. Hajdukiewicz, M. Geron, and M. M. Keane, "Formal calibration methodology for CFD models of naturally ventilated indoor environments," *Build. Environ.*, vol. 59, pp. 290–302, 2012.

[17] M. Hajdukiewicz, M. Geron, and M. M. Keane, "Calibrated CFD simulation to evaluate thermal comfort in a highly-glazed naturally ventilated room," *Build. Environ.*, vol. 70, pp. 73–89, 2013.

[18] X. Wang, X. Wang, G. Xing, J. Chen, C.-X. Lin, and Y. Chen, "Towards Optimal Sensor Placement for Hot Server Detection in Data Centers," in *2011 31st International Conference on Distributed Computing Systems*, 2011, pp. 899–908.

[19] Z. Bai, P. M. Dewilde, and R. W. Freund, *Numerical Methods in Electromagnetics*, vol. 13. Elsevier, 2005, pp. 825–895.

*Corresponding Author: Marco Geron, School of Mechanical and Aerospace Engineering, Queen's University Belfast, Belfast, UK. Tel:+442890424728. E-mail address: m.geron@qub.ac.uk

[20] M. Geron, C. Butler, J. Stafford, and D. Newport, "Development and Validation of a Compact Thermal Model for an Aircraft Compartment," *Appl. Therm. Eng.*, no. 61, pp. 65–74, 2013.

[21] A. C. Megri and F. Haghighat, "Zonal Modeling for Simulating Indoor Environment of Buildings: Review, Recent Developments, and Applications," *HVAC&R Res.*, vol. 13, no. 6, pp. 887–905, Nov. 2007.

[22] C. Farhat and D. Amsallem, "REDUCED-ORDER MODELING , DIFFERENTIAL GEOMETRY AND PHYSICS-BASED NEAR-REAL-TIME PREDICTIONS," vol. 195, no. Eccomas, p. 5742, 2008.

[23] S. Goyal and P. Barooah, "A method for model-reduction of non-linear thermal dynamics of multi-zone buildings," *Energy Build.*, vol. 47, pp. 332–340, Apr. 2012.

[24] M. Geron, R. F. D. Monaghan, M. M. Keane, and M. M. K. M. Geron, R.F.D. Monaghan, "REDUCED ORDER MODELLING OF THE THERMAL BEHAVIOUR OF AN OFFICE SPACE," in *International Conference Cleantech for smart cities & building from nano to urban scale*, 2013, no. 1.

[25] R. F. D. Monaghan, A. Cuoci, G. Bourque, M. Fu, R. L. Gordon, T. Faravelli, A. Frassoldati, and H. J. Curran, "Detailed Multi-dimensional Study of Pollutant Formation in a Methane Diffusion Flame," *Energy Fuels*, vol. 26, no. 3, pp. 1598–1611, 2012.

[26] Onset, "Onset HOBO Data Loggers." [Online]. Available: http://www.onsetcomp.com/products.

[27] *PHOENICS' user manual*. CHAM ltd., 2011, p. 328.

[28] M. Hajdukiewicz, M. Geron, and M. M. Keane, "Evaluation of Various Turbulence Models to Predict Indoor Conditions in a Naturally Ventilated Room," in *11th REHVA World Congress & 8th International Conference on IAQVEC, CLIMA2013*, 2013, vol. 59, pp. 290–302.

[29] *Tecplot CFD post processing tools visualize & analyze data results*. Amtec Engineering, Incorporated, 2013, p. 628.

[30] B. A. Cullimore, S. G. Ring, and D. A. Johnson, *General Purpose Thermal/Fluid Network Analyzer V5.5*. C&R Technologies, Inc. ("CRTech"), 2011.

[31] "CS 294-74: Mesh Generation and Geometry Processing." .

*Corresponding Author: Marco Geron, School of Mechanical and Aerospace Engineering, Queen's University Belfast, Belfast, UK. Tel:+442890424728. E-mail address: m.geron@qub.ac.uk

Figure 1 Numerical and physical domain ..... **Error! Bookmark not defined.**
Figure 2: Wireless sensor distribution in the office space ..... **Error! Bookmark not defined.**
Figure 3: Grid convergence analysis for three temperature profiles along the North-South direction .... **Error! Bookmark not defined.**
Figure 4 Temperature recorded at one point at the ceiling, wall and air temperature during a cooling down (Radiators off, door and windows opened) experiment. ..... **Error! Bookmark not defined.**
Figure 5 Validation of the CFD base models ..... **Error! Bookmark not defined.**
Figure 6 Integration of automatically extracted ROMs into the BEMS ..... **Error! Bookmark not defined.**
Figure 7 Flow chart of the ROM extraction method ..... **Error! Bookmark not defined.**
Figure 8 Examples of the application of a zoning criterion (temperature), two criterion increments (panels (a)-(c) show 2 ^{o}C and panels (d)-(f) show 1 ^{o}C), which produce the zone-types and zones displayed. Zone-types can be non-unique while zones must be unique. ..... **Error! Bookmark not defined.**
Figure 9 Graphical representation of creating a zone ..... **Error! Bookmark not defined.**
Figure 10 Sample path of the creation of a set of zones ..... **Error! Bookmark not defined.**
Figure 11 Zone-Zone interface ..... **Error! Bookmark not defined.**
Figure 12 CFD-predicted 3D temperature contours ..... **Error! Bookmark not defined.**
Figure 13 5-zone ROM-predicted 3D temperature contours ..... **Error! Bookmark not defined.**
Figure 14 9-zone ROM-predicted 3D temperature contours ..... **Error! Bookmark not defined.**
Figure 15 33-zone ROM-predicted 3D temperature contours ..... **Error! Bookmark not defined.**
Figure 16 Impact of ROM size on E_t and time to solution ..... **Error! Bookmark not defined.**
Figure 17 Multi CFD approach verses the Multi ROM approach ..... **Error! Bookmark not defined.**
Figure 18 Contour plot of EMR for case C1W0D1 (Tc+5^{o}C) ..... **Error! Bookmark not defined.**
Figure 19 Contour plot of EMR for case C1W1D1 (Tw-5^{o}C) ..... **Error! Bookmark not defined.**
Figure 20 Plot of EMR for case C0W1D1 (Tw-5^{o}C) ..... **Error! Bookmark not defined.**

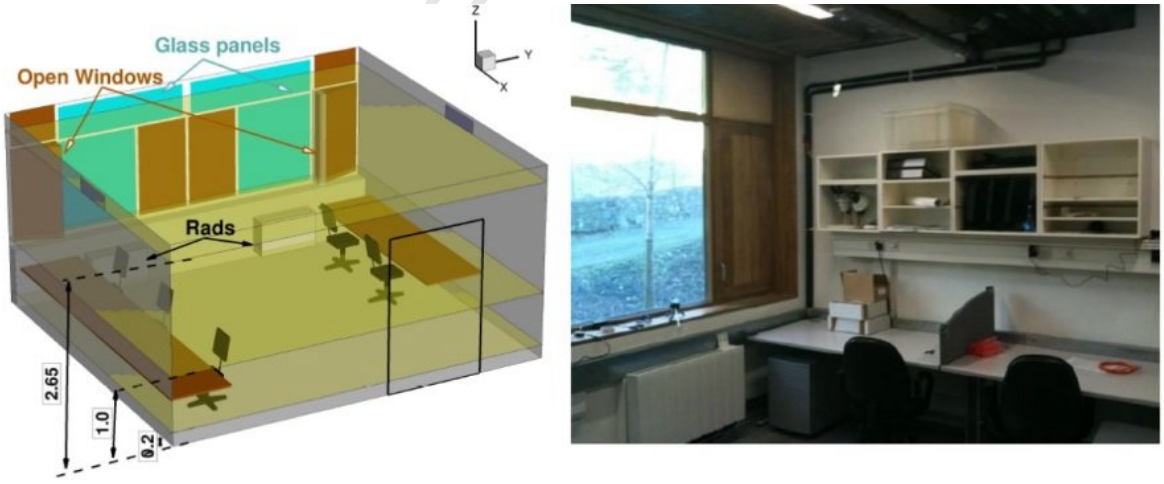

Figure 1 Numerical and physical domain

*Corresponding Author: Marco Geron, School of Mechanical and Aerospace Engineering, Queen's University Belfast, Belfast, UK. Tel:+442890424728. E-mail address: m.geron@qub.ac.uk

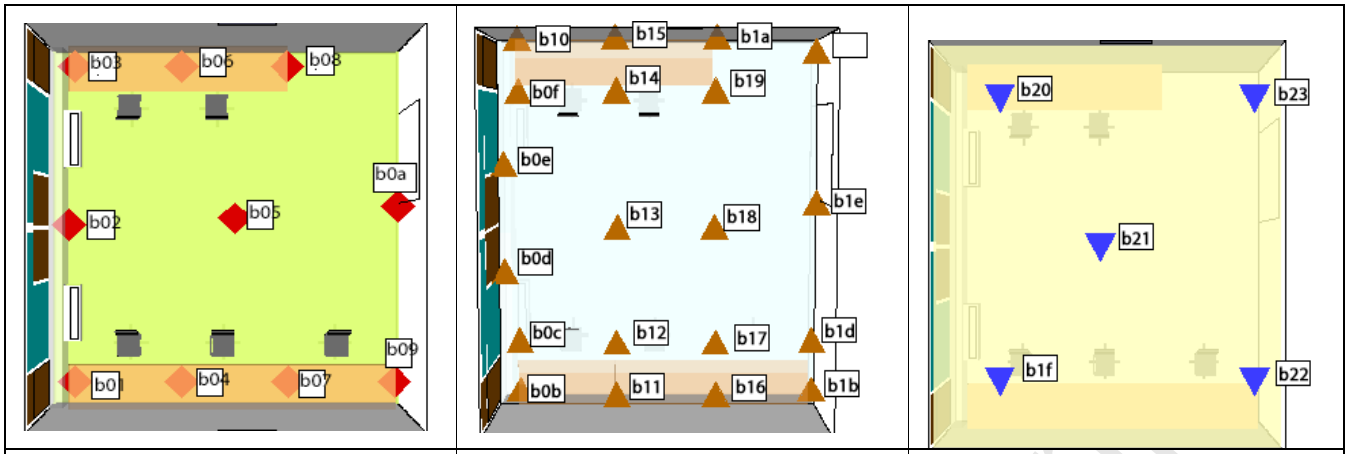

a) Floor Level | b) User Level | c) Ceiling Level

Figure 2: Wireless sensor distribution in the office space

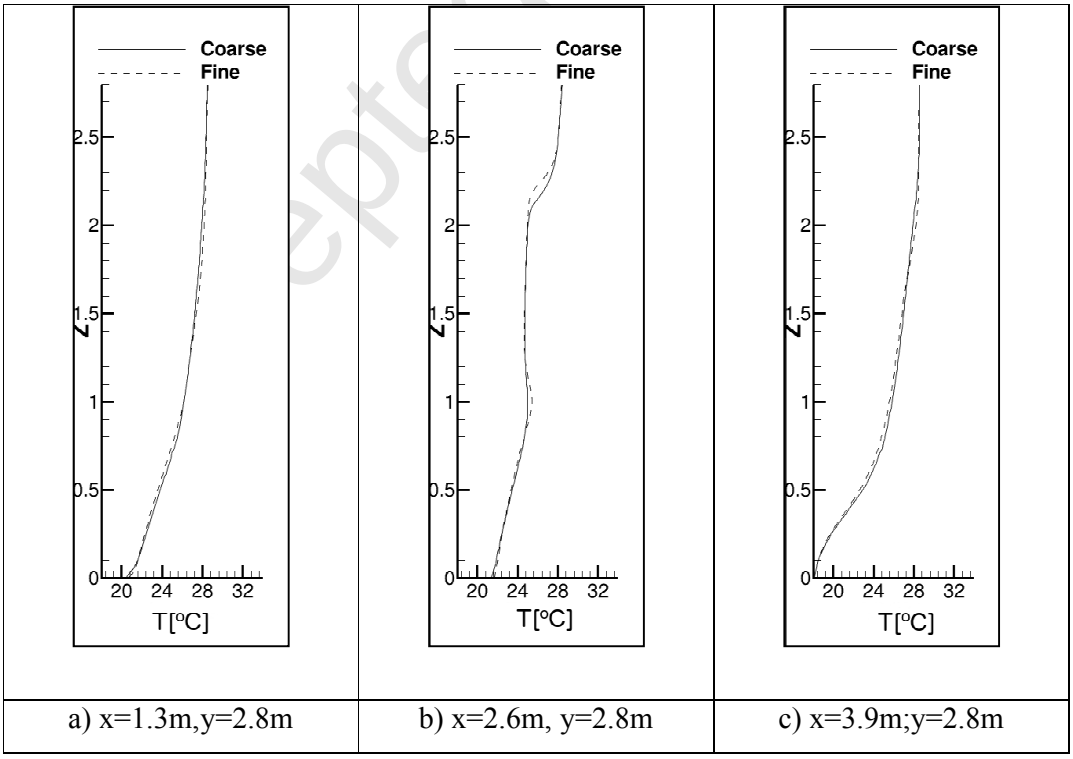

a) x=1.3m,y=2.8m | b) x=2.6m, y=2.8m | c) x=3.9m;y=2.8m

Figure 3: Grid convergence analysis for three temperature profiles along the North-South direction

*Corresponding Author: Marco Geron, School of Mechanical and Aerospace Engineering, Queen's University Belfast, Belfast, UK. Tel:+442890424728. E-mail address: m.geron@qub.ac.uk

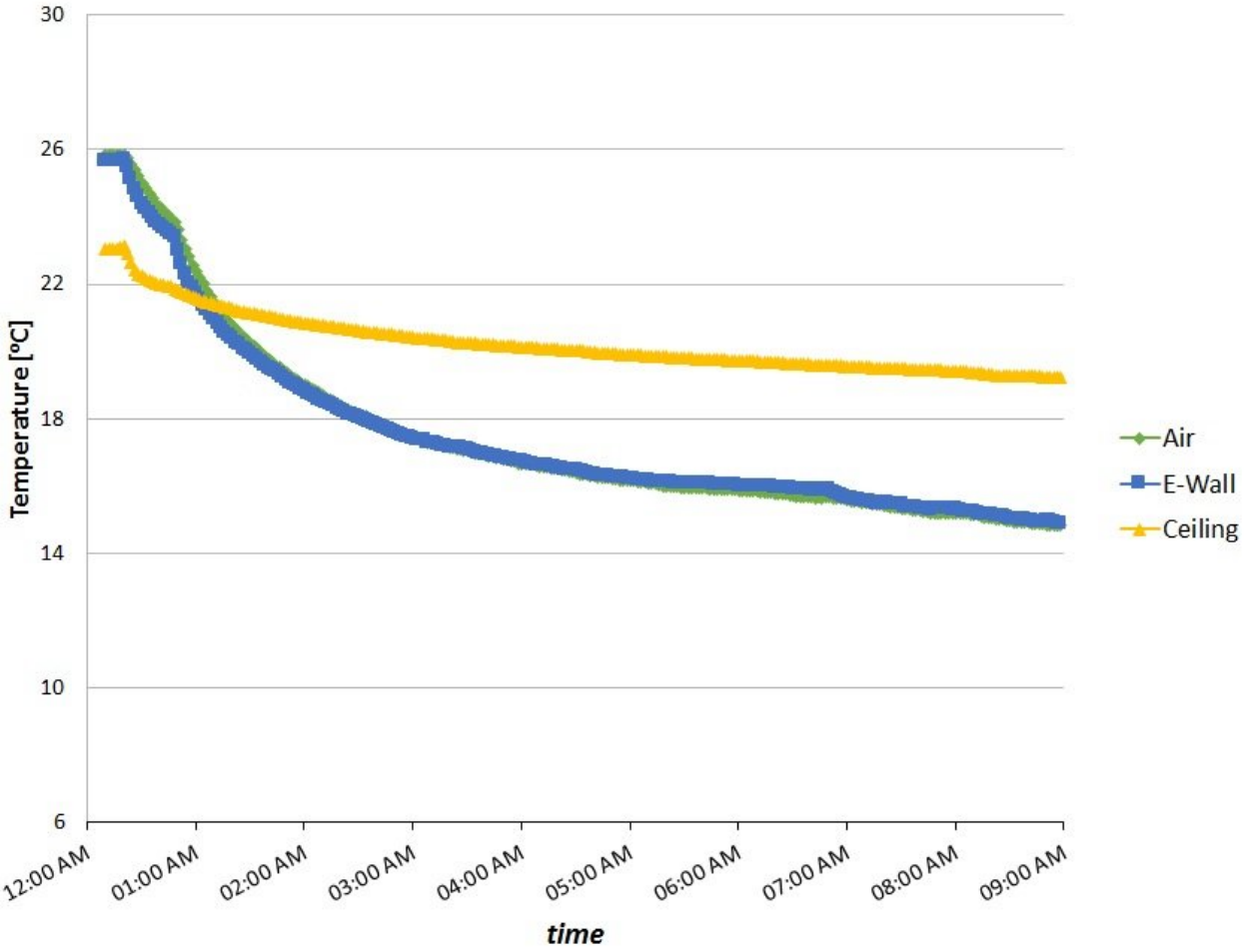

Figure 4 Temperature recorded at one point at the ceiling, wall and air temperature during a cooling down (Radiators off, door and windows opened) experiment.

*Corresponding Author: Marco Geron, School of Mechanical and Aerospace Engineering, Queen's University Belfast, Belfast, UK. Tel:+442890424728. E-mail address: m.geron@qub.ac.uk

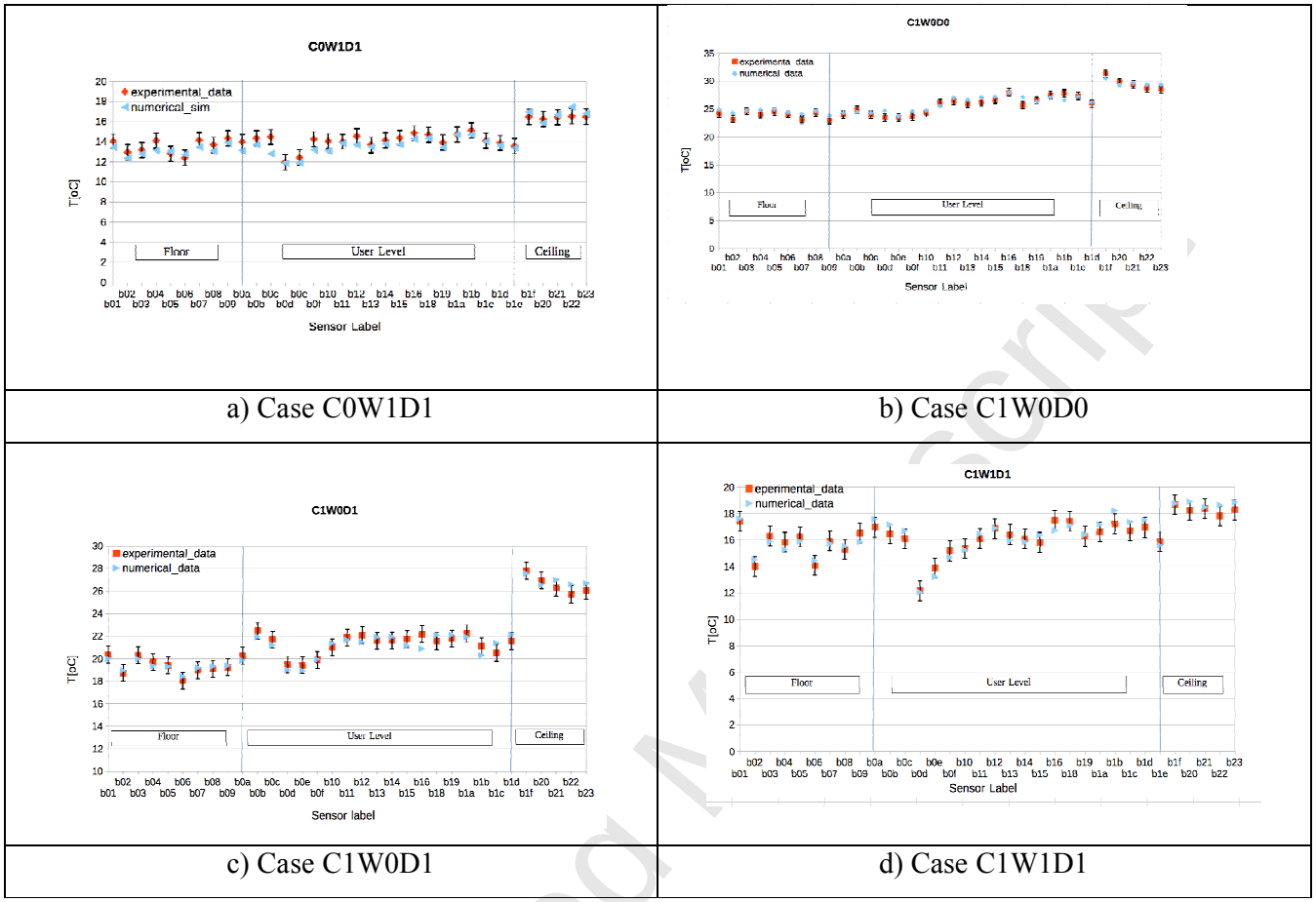

a) Case C0W1D1 b) Case C1W0D0

c) Case C1W0D1 d) Case C1W1D1

Figure 5 Validation of the CFD base models

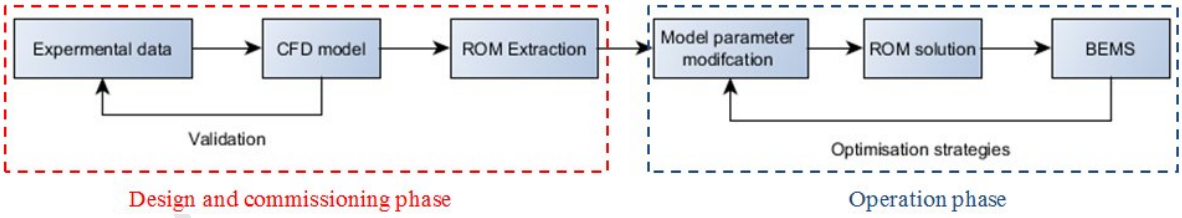

Figure 6 Integration of automatically extracted ROMs into the BEMS

*Corresponding Author: Marco Geron, School of Mechanical and Aerospace Engineering, Queen's University Belfast, Belfast, UK. Tel:+442890424728. E-mail address: m.geron@qub.ac.uk

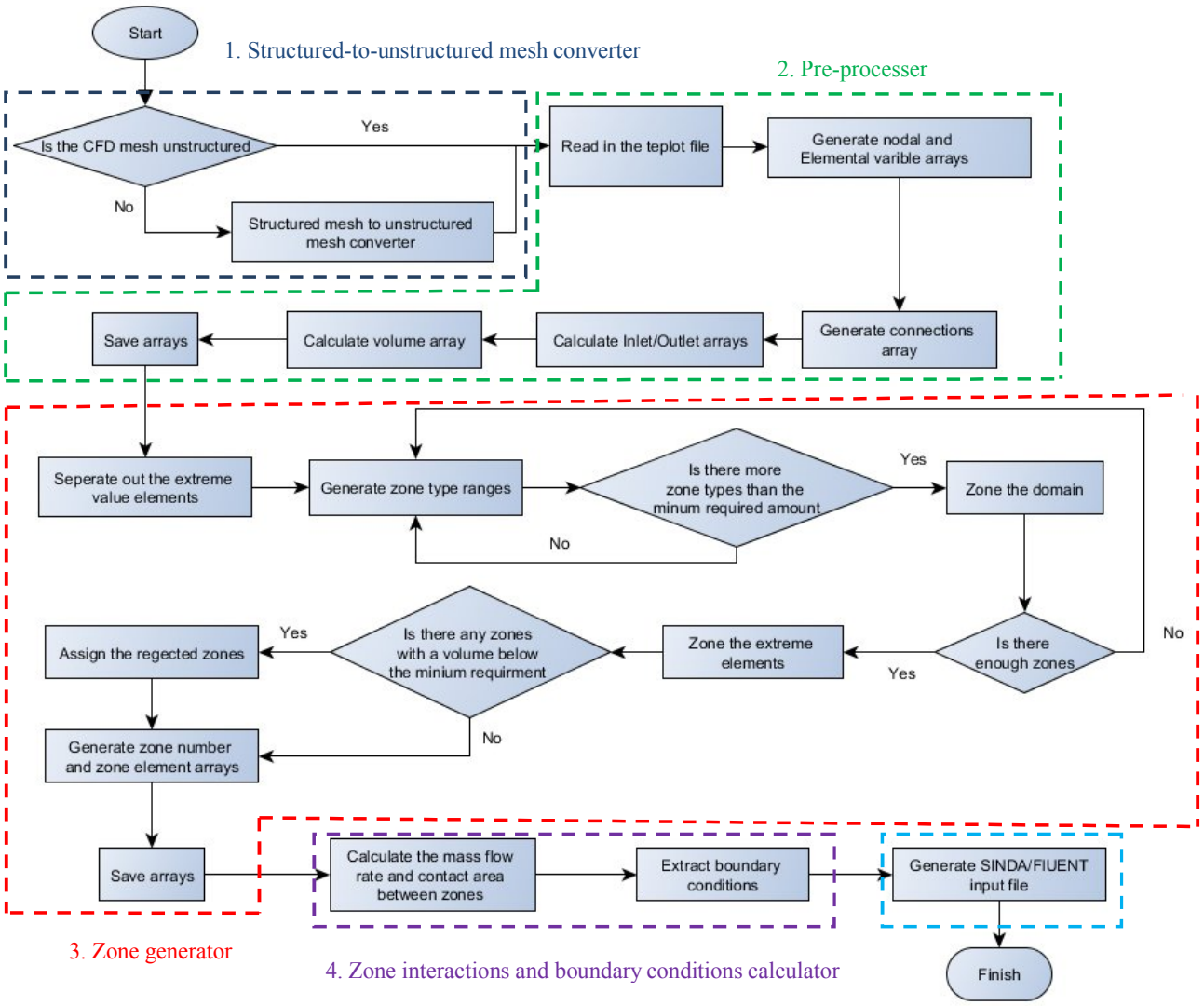

Figure 7 Flow chart of the ROM extraction method

*Corresponding Author: Marco Geron, School of Mechanical and Aerospace Engineering, Queen's University Belfast, Belfast, UK. Tel:+442890424728. E-mail address: m.geron@qub.ac.uk

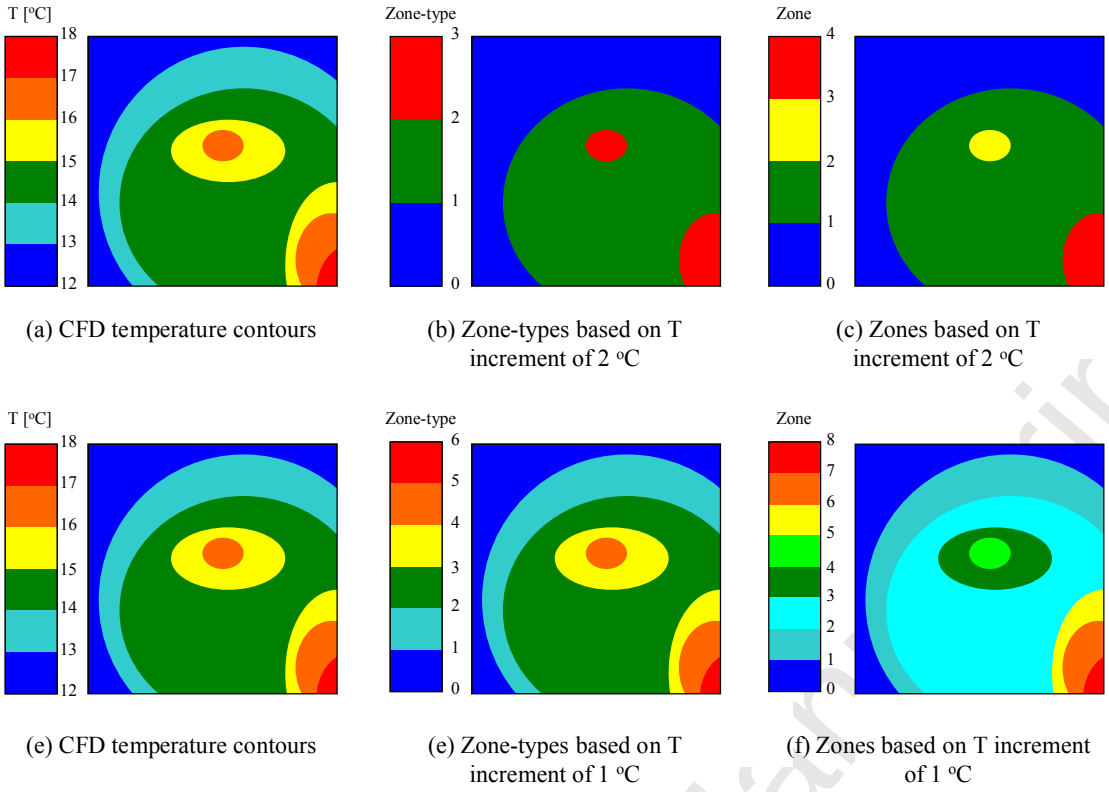

(a) CFD temperature contours

(b) Zone-types based on T increment of 2 ºC

(c) Zones based on T increment of 2 ºC

(e) CFD temperature contours

(e) Zone-types based on T increment of 1 ºC

(f) Zones based on T increment of 1 ºC

Figure 8 Examples of the application of a zoning criterion (temperature), two criterion increments (panels (a)-(c) show 2 ºC and panels (d)-(f) show 1 ºC), which produce the zone-types and zones displayed. Zone-types can be non-unique while zones must be unique.

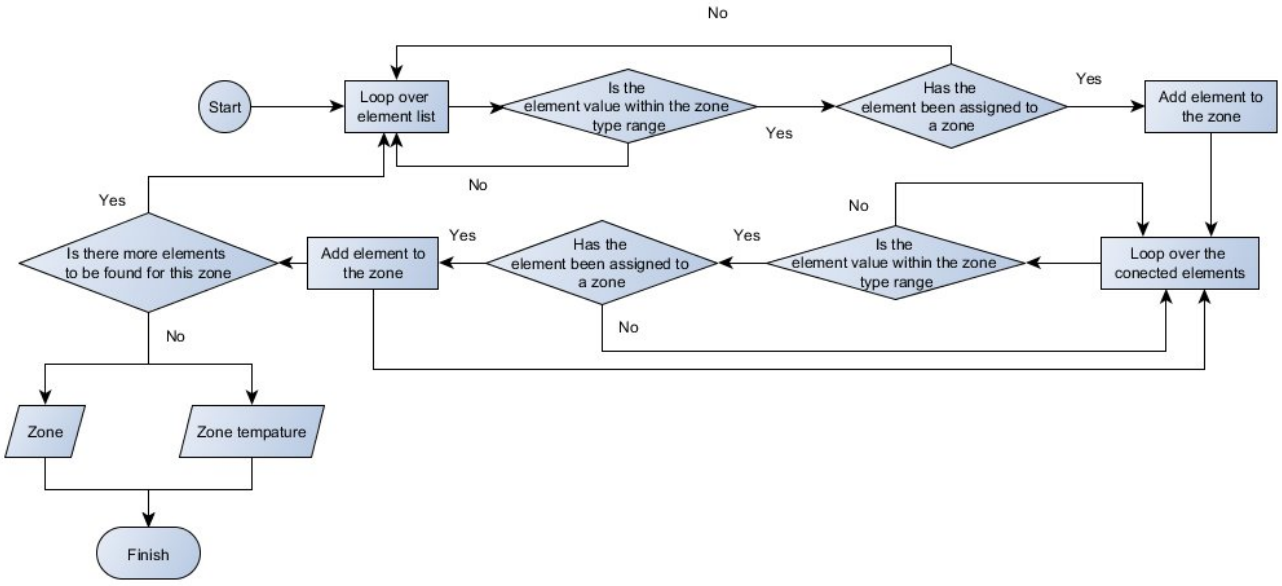

Figure 9 Graphical representation of creating a zone

*Corresponding Author: Marco Geron, School of Mechanical and Aerospace Engineering, Queen's University Belfast, Belfast, UK. Tel:+442890424728. E-mail address: m.geron@qub.ac.uk

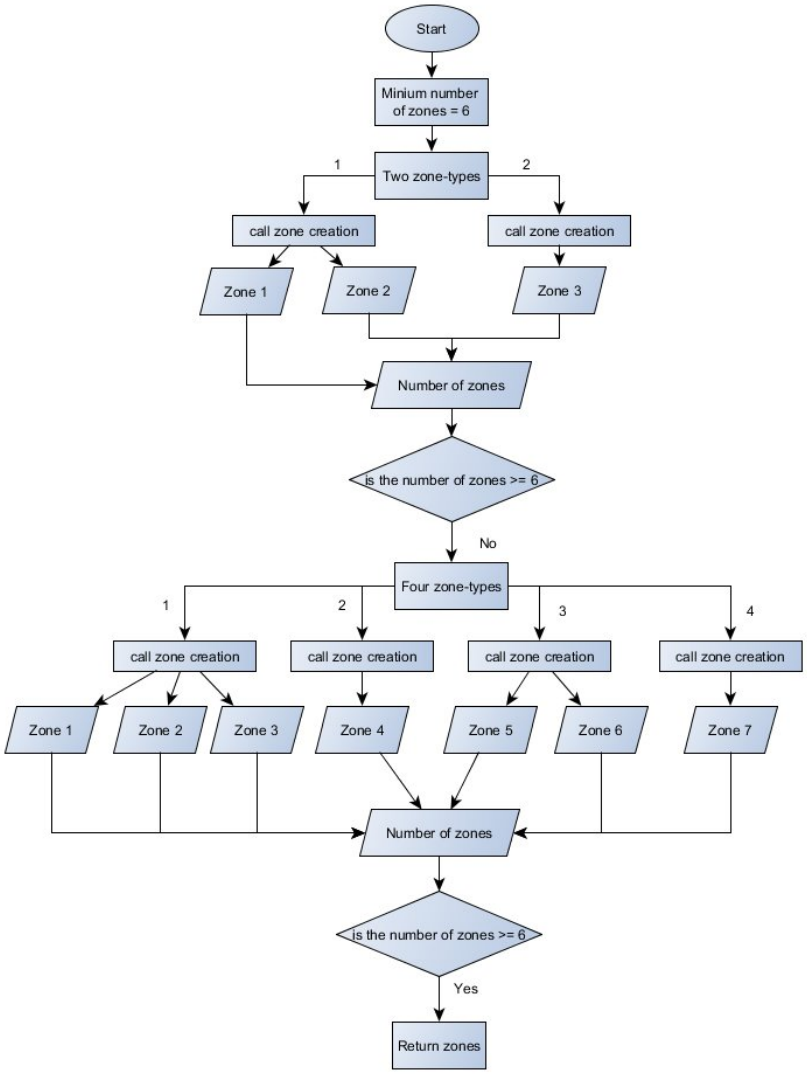

Figure 10 Sample path of the creation of a set of zones

*Corresponding Author: Marco Geron, School of Mechanical and Aerospace Engineering, Queen's University Belfast, Belfast, UK. Tel:+442890424728. E-mail address: m.geron@qub.ac.uk

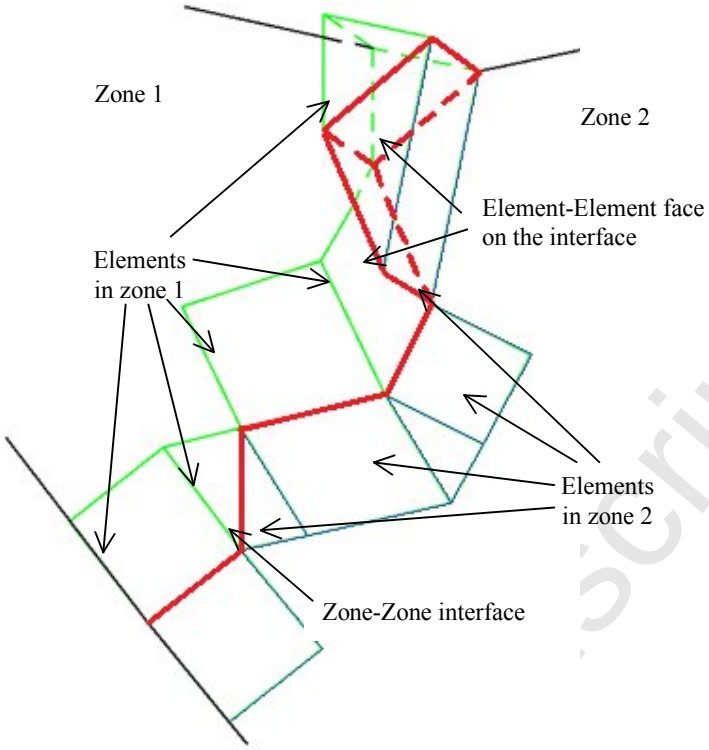

Figure 11 Zone-Zone interface

*Corresponding Author: Marco Geron, School of Mechanical and Aerospace Engineering, Queen's University Belfast, Belfast, UK. Tel:+442890424728. E-mail address: m.geron@qub.ac.uk

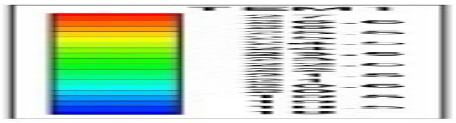

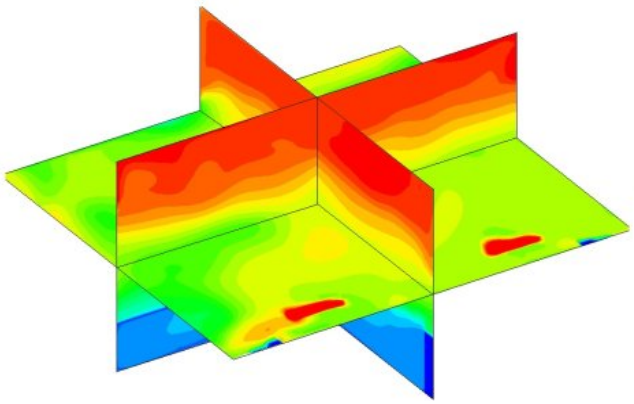

Figure 12 CFD-predicted 3D temperature contours

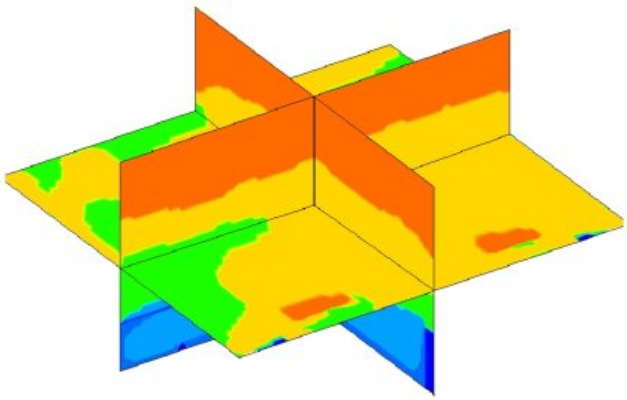

Figure 13 5-zone ROM-predicted 3D temperature contours

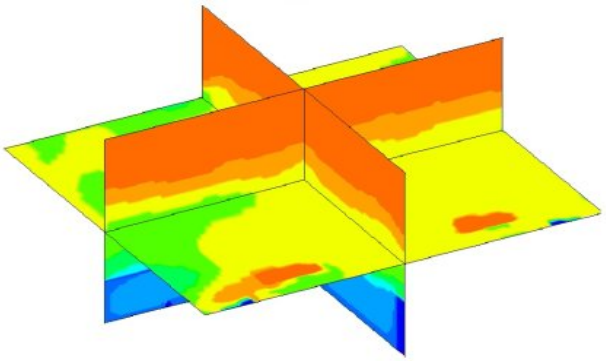

Figure 14 9-zone ROM-predicted 3D temperature contours

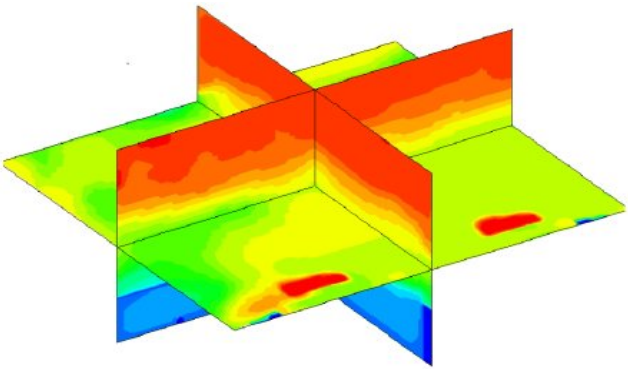

Figure 15 33-zone ROM-predicted 3D temperature contours

*Corresponding Author: Marco Geron, School of Mechanical and Aerospace Engineering, Queen's University Belfast, Belfast, UK. Tel:+442890424728. E-mail address: m.geron@qub.ac.uk

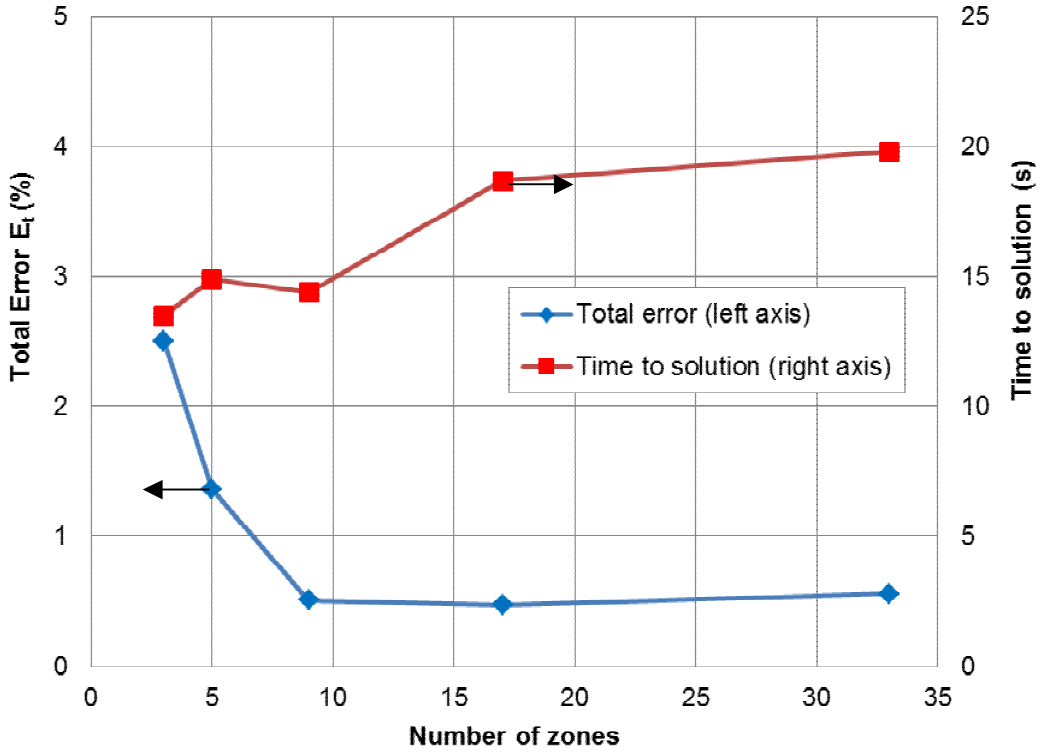

Figure 16 Impact of ROM size on E_t and time to solution

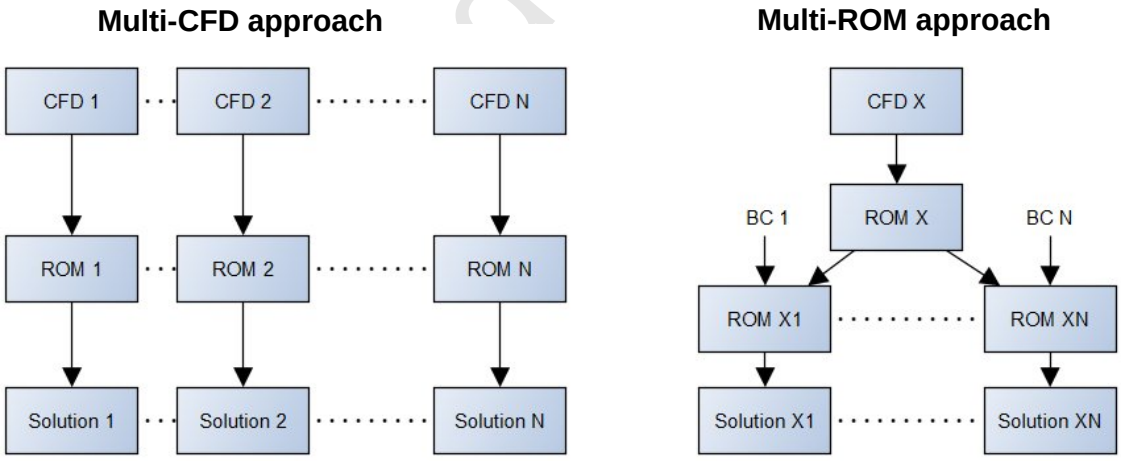

Figure 17 Multi CFD approach verses the Multi ROM approach

*Corresponding Author: Marco Geron, School of Mechanical and Aerospace Engineering, Queen's University Belfast, Belfast, UK. Tel:+442890424728. E-mail address: m.geron@qub.ac.uk

Table 1 Matrix of CFD simulations

Case	Boundary condition	T_C (^oC)	T_W (^oC)	Et (%)
C1W0D0	Base	45	N/A	3.4
	$T_C + 5^oC$	50	N/A	3.53
	$T_C - 5^oC$	40	N/A	3.27
C0W1D1	Base	N/A	12	1.36
	$T_W + 5^oC$	N/A	17	0.41
	$T_W - 5^oC$	N/A	7	1.64
C1W0D1	Base	45	N/A	0.99
	$T_C + 5^oC$	50	N/A	1.48
	$T_C - 5^oC$	40	N/A	2.87
C1W1D1	Base	45	9	2.86
	$T_C + 5^oC$	50	9	3.25
	$T_C - 5^oC$	40	9	1.63
	$T_W + 5^oC$	45	14	4.83
	$T_W - 5^oC$	45	4	3.20

Table 2 Multi-CFD and Multi-ROM comparison

Case	Boundary condition	E_t (%) Multi-CFD	E_t (%) Multi-ROM	E_{MR}
C1W0D0	$T_C + 5^oC$	3.53	8.45	4.98
	$T_C - 5^oC$	3.27	3.76	5.75
C0W1D1	$T_W + 5^oC$	0.41	7.54	8.43
	$T_W - 5^oC$	1.64	8.11	8.33
C1W0D1	$T_C + 5^oC$	1.48	2.41	1.42
	$T_C - 5^oC$	2.87	3.40	5.72
C1W1D1	$T_C + 5^oC$	3.25	2.99	1.46
	$T_C - 5^oC$	1.63	7.57	8.16
	$T_W + 5^oC$	4.83	9.86	6.54
	$T_W - 5^oC$	3.20	8.14	4.94

*Corresponding Author: Marco Geron, School of Mechanical and Aerospace Engineering, Queen's University Belfast, Belfast, UK. Tel:+442890424728. E-mail address: m.geron@qub.ac.uk

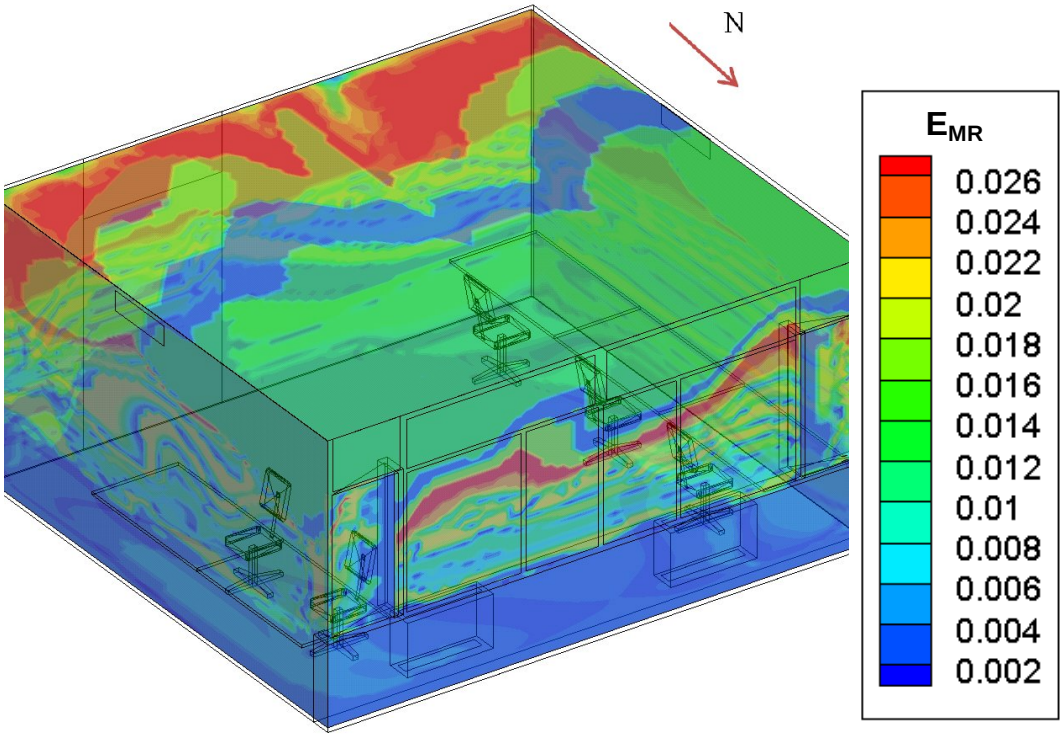

Figure 18 Contour plot of EMR for case C1W0D1 (Tc+5°C)

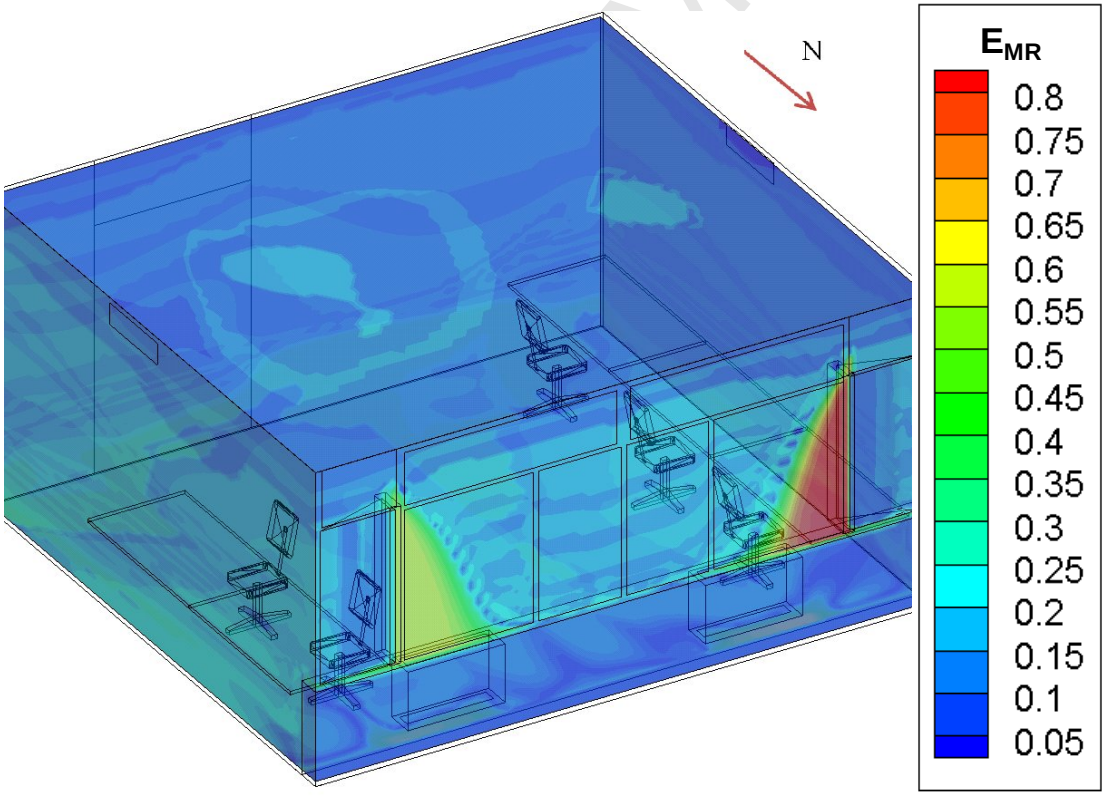

Figure 19 Contour plot of EMR for case C1W1D1 (Tw-5°C)

*Corresponding Author: Marco Geron, School of Mechanical and Aerospace Engineering, Queen's University Belfast, Belfast, UK. Tel:+442890424728. E-mail address: m.geron@qub.ac.uk

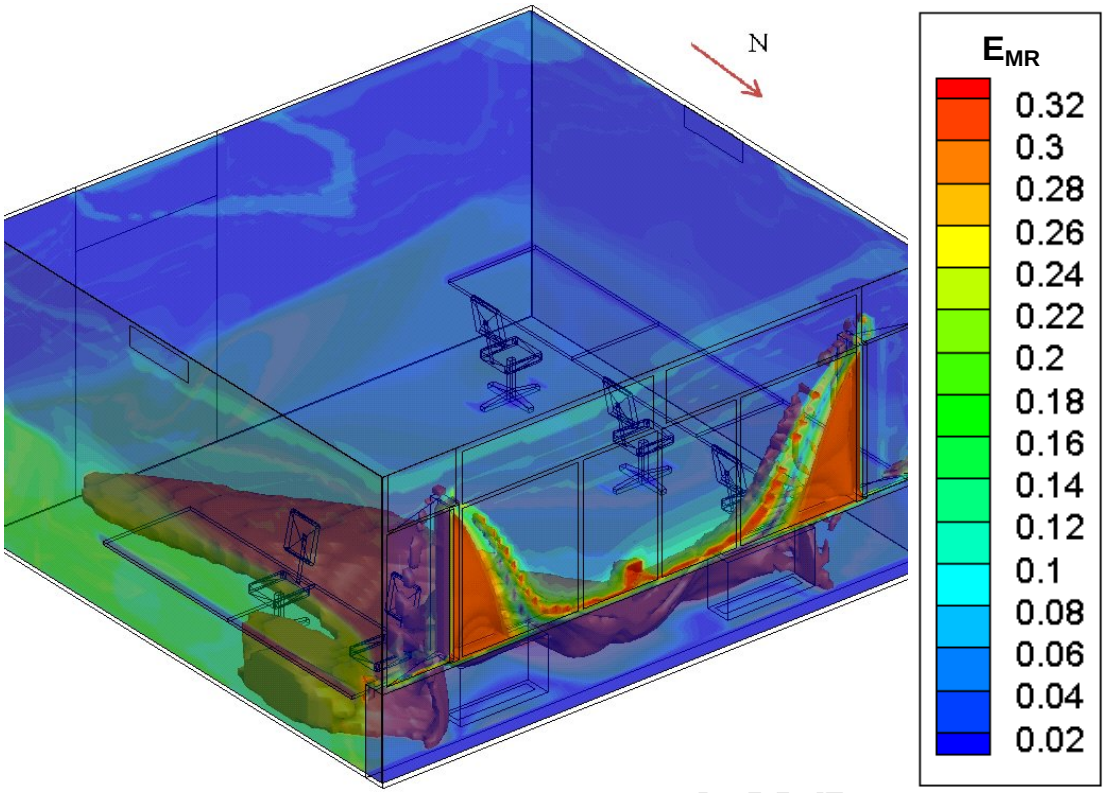

Figure 20 Plot of EMR for case C0W1D1 (Tw-5^{o}C)

*Corresponding Author: Marco Geron, School of Mechanical and Aerospace Engineering, Queen's University Belfast, Belfast, UK. Tel:+442890424728. E-mail address: m.geron@qub.ac.uk